Processing Techniques for Nadir Echo Suppression in Staggered Synthetic Aperture Radar

Maxwell Nogueira Peixoto and Michelangelo Villano, *Senior Member, IEEE*

***Abstract*—Synthetic aperture radar (SAR) is a class of high-resolution imaging radar particularly suitable for satellite remote sensing with diverse applications such as biomass and ice monitoring, generation of digital elevation models, and measuring of subsidence. Staggered SAR is a novel mode of operation under consideration for next-generation SAR missions such as Tandem-L and NASA-ISRO SAR. It uses digital beamforming and a continuous variation of the pulse repetition interval (PRI) to achieve high azimuth resolution over a much wider, continuous swath than is traditionally possible. This PRI variation renders infeasible the use of existing methods to avoid nadir echoes, which might impair the quality of staggered SAR images. This work proposes processing techniques that mitigate the impact of nadir echoes in staggered SAR through localization and thresholding-and-blanking of these echoes in range-compressed data and recovery of part of the underlying useful signal through interpolation. The performance of these processing techniques is evaluated through simulations using real TerraSAR-X data. The proposed technique can be implemented as an optional stage in the processing chain of future staggered SAR missions and leads to improved image quality at a reasonable additional computational cost.**

***Index Terms*—High-resolution wide-swath (HRWS) imaging, multiple-elevation-beam SAR, nadir echo, NASA-ISRO SAR (NISAR), staggered SAR, synthetic aperture radar (SAR), Tandem-L.**

I. Introduction

Synthetic aperture radar (SAR) is a class of high-resolution imaging radar that is particularly suitable for satellite remote sensing, especially for applications that use time series, as it can operate regardless of weather or sunlight presence. Being able to image even wider swaths is desirable for it allows ever lower revisit times, which is crucial for applications studying dynamic systems of the planet [1], [2]. Under traditional SAR systems, wider swaths are only attainable at the cost of lower azimuth resolution. Multiple-elevation-beam SAR surpasses this trade-off though the use of digital beamforming to simultaneously image multiple sub-swaths, achieving a much wider swath than is traditionally possible for the same azimuth resolution [1].

SAR conventionally operates by transmitting pulses at regular intervals, the pulse repetition interval (PRI). In a SAR with multiple elevation beams and a constant PRI, this regularity causes some ranges inside the swath to never be imaged. They are called “blind ranges”. Staggered SAR is a novel mode of operation that overcomes this by changing the PRI every pulse so the blind ranges change position every pulse and, with sufficient oversampling, can be interpolated over to achieve a wide continuous swath [2]-[5]. This mode is under consideration for next-generation satellite missions such as Tandem-L and NASA-ISRO SAR (NISAR) [2]-[8].

The pulse-to-pulse variation of the PRI means that staggered SAR raw data are non-uniformly sampled in the azimuth direction, and the blind ranges correspond to gaps in these data. To process these data into a focused image, one can first resample it into a uniform grid and then apply conventional SAR processing. The resampling can be performed through best linear unbiased (BLU) interpolation of neighboring correlated samples, and the best performance of this processing scheme is achieved when data are oversampled in azimuth by a factor of around 1.5 to 2 higher than for constant PRI SAR [2], [4], [5].

Nadir echoes are the echoes caused by reflection in the nadir direction. They arrive superimposed to and corrupt echoes from the imaged swath. Even though the antenna pattern only faintly illuminates the nadir, nadir echoes can be exceptionally strong due to specular reflection but are also very localized in the form of a sharp peak followed by a long tail. In constant PRI SAR, they appear at the same slant ranges for every pulse, corrupting the SAR images in the form of a bright line (cf. Fig. 1 (a)), and are generally avoided by selecting, through a timing diagram, a pulse repetition frequency (PRF) that causes them to be contained in the blind ranges.

As discussed in detail in [9], the PRI variation in staggered SAR causes nadir echoes of each pulse to be located at different slant ranges, rendering the common approach to avoid them unfeasible. Their positioning in the raw or range-compressed data can be derived from the PRI sequence employed and the

Manuscript received December, 2021; revised Month XX, 202X; accepted Month XX, 202X. Date of publication Month XX, 202X; date of current version Month XX, 202X.

The authors are with the German Aerospace Center (DLR), Microwaves and Radar Institute Oberpfaffenhofen, 82234 Wessling, Germany (e-mail: Maxwell.NogueiraPeixoto@dlr.de).

Color versions of one or more of the figures in this paper are available online at http://ieeexplore.ieee.org.

Digital Object Identifier XX.XXXX/TGRS.202X.XXXXXXX.

distance to the nadir, and can be visualized through the nadir echo location diagram (an example is show in Fig. 2) [9]. The ambiguity order of a nadir echo in raw or range-compressed data is the number of pulses between the pulse that generated the nadir echo and the pulse that corresponds to the range line in which the nadir echo was received. As is clear in Fig. 2, the nadir echoes are grouped into clusters, each over a well-defined slant range interval and identified by the echoes' common ambiguity order. The azimuth compression "smears" them along azimuth, so they then appear as various azimuth stripes over each cluster's slant range interval in staggered SAR images (cf. Fig. 1 (b)).

The smearing and, as the raw data are oversampled, Doppler filtering provide a strong attenuation of the peak nadir echo intensity in staggered SAR images [9], [10]. Even so, in some cases, the nadir echoes may still be much stronger than the noise level and significantly impair the image quality, which prompts for the development of methods of identifying and further suppressing them [9], [10].

This paper proposes a thresholding-and-blanking approach to suppress nadir echoes in staggered SAR that can be integrated in the SAR processing chain and does not require any system changes. An alternative to this approach is also presented that leverages the azimuth oversampling of the data to recover part of the useful signal destroyed by the blanking. The performance of these techniques is then evaluated through simulations using real TerraSAR-X data.

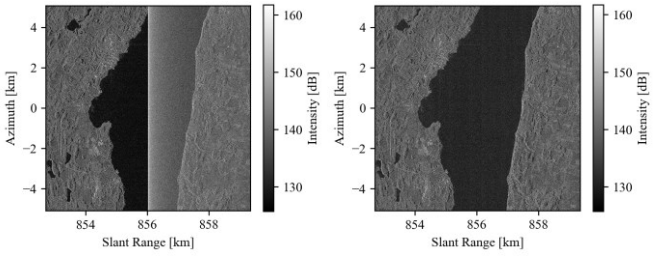

Fig. 1. Simulated (a) conventional and (b) staggered SAR images over lake Starnberg including strong nadir echo, which appears "smeared" in the staggered SAR case.

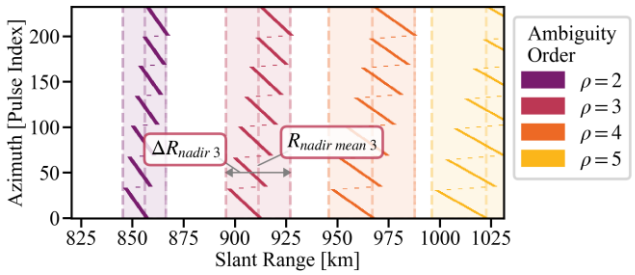

Fig. 2. An example of nadir echo location diagram for Tandem-L over its swath. This diagram repeats itself periodically along azimuth.

II. Nadir Echo Suppression by Thresholding and Blanking

Nadir echoes in staggered SAR data can be suppressed though a thresholding-and-blanking processing step by exploiting the knowledge of their position. This processing step is performed before staggered SAR raw data are resampled onto a uniform grid. First, data are range-compressed, and nadir echoes are aligned and averaged to obtain a speckle-free profile. This profile is then compared against a threshold, and the nadir echo samples which exceed the threshold are blanked. Finally, an inverse range compression is performed, and the resulting data are processed into an image by a staggered SAR processor [4]. This method is suitable for staggered SAR because the positions of the nadir echoes are roughly known, and errors introduced by the blanking end up smeared over large spans in range in the same way the nadir echoes would in case no suppression was performed.

Nadir echoes are blanked in range-compressed data, as, at this stage, they occupy the least number of samples and so the blanking removes the smallest amount of underlying useful signal. If the blanking were performed after azimuth compression, the nadir echoes would be smeared over the entire synthetic aperture. Similarly, if it were performed after resampling the staggered SAR raw data onto a regular grid, the resampling would still smear each nadir echo over a few samples along azimuth. Finally, in the raw data, each nadir echo occupies several pixels in range as it is convolved with the pulse waveform of the system.

As depicted in Fig. 3, the processing pipeline must be changed to first range-compress the raw data, then blank the nadir echoes in the range-compressed data, then return to the raw data by inverse range compression, and only then resample and focus the data. The inverse range compression is needed because the resampling is optimally done in the raw data [4].

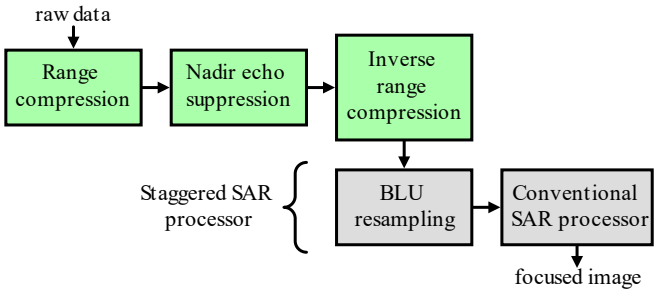

Fig. 3. Block diagram of the processing of staggered SAR raw data into a focused image including the nadir echo suppression. The green blocks are responsible for nadir echo suppression.

A. Backscatter Profile Estimate

The staggered range-compressed data are aligned and averaged along azimuth to estimate the profile of nadir echo backscatter along range. This profile will be used to decide which samples are to be blanked. Averaging is needed because nadir echoes contain speckle, so the decision of whether to blank a sample with nadir echo cannot be made based solely on the value of that individual sample.

In staggered SAR, the nadir echoes appear at different slant ranges for different range lines, so matching range translations must be applied to the data prior to averaging. More precisely, to obtain the backscatter profile estimate for nadir echoes of ambiguity order ρ based on N range lines starting from that of

index k_0, one must evaluate the backscatter profile in the range-compressed data $\widehat{\sigma_\rho^0}(R)$

$$\widehat{\sigma_\rho^0}(R) = \frac{1}{N}\sum_{k=k_0}^{k_0+N-1} \left|s_{RC}\left(R + R_{nadir\ \rho,k} - h, k\right)\right|^2 \quad (1)$$

for values of slant range R over a reasonably large interval surrounding h, where h is the height of the radar platform, $s_{RC}(R,k)$ is the staggered SAR range-compressed data for the slant range R at the range line of index k, and $R_{nadir\ \rho,k}$ is the slant range of the nadir echo of ambiguity order ρ at the range line of index k (a formula for $R_{nadir\ \rho,k}$ is presented in [9]). Note that the data being averaged is the superposition of the nadir echoes and the useful signal, so $\widehat{\sigma_\rho^0}(R)$ must then be decomposed into $\widehat{\sigma_\rho^0}_{useful}$, a constant "background" level corresponding to the useful signal, and $\widehat{\sigma_\rho^0}_{nadir}(R)$, the "spike" above the useful signal level which is identified as corresponding to the nadir echo:

$$\widehat{\sigma_\rho^0}(R) = \widehat{\sigma_\rho^0}_{useful} + \widehat{\sigma_\rho^0}_{nadir}(R). \quad (2)$$

Fig. 4 shows an example of backscatter profile estimate (blue) and its background level (black, dashed). If the nadir topography is fast-changing, the estimated profile will be smeared, possibly incurring in lower nadir echo suppression.

It is worth remarking that the range translations in (1), which align the nadir echoes, misalign the underlying useful signal. The estimate $\widehat{\sigma_\rho^0}(R)$ for any specific R then includes a useful signal component given by the average of useful signal samples from vastly different slant ranges spanning the same size of the slant range interval affected by the respective cluster of nadir echoes (cf. Fig. 2).

B. Thresholding and Blanking

The backscatter profile estimate is compared to a threshold, which, in the simplest approach, is set to twice the useful signal level $\widehat{\sigma_\rho^0}_{useful}$, and all samples corresponding to when it is exceeded are blanked.

Blanking a sample completely removes its nadir echo, but also removes the useful signal in it, which introduces errors into the focused image. The simplest criterion for selecting the blanking threshold is then to blank only the samples whose nadir echo is stronger than the underlying useful signal, otherwise the error introduced by the blanking would be larger than the removed nadir disturbance. This translates to setting the threshold to twice the useful signal level $\widehat{\sigma_\rho^0}_{useful}$ in the backscatter estimate.

Comparing the backscatter estimate with the blanking threshold yields, as depicted in Fig. 4, the slant range interval $\mathcal{R}_{blank}$ marking where the threshold is exceeded. The samples to be blanked are then all those for which

$$R - R_{nadir\ \rho,k} + h \in \mathcal{R}_{blank}, \quad (3)$$

where R is the sample's slant range, k is index of the sample's range line, and $R_{nadir\ \rho,k}$ and h are as in (1).

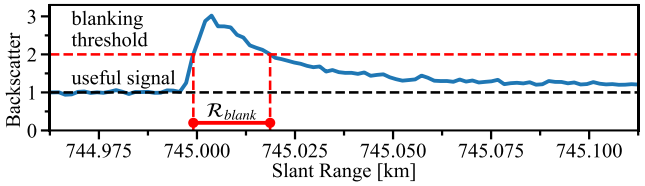

Fig. 4. Example of a backscatter profile estimate for nadir echoes of ambiguity order $\rho = 2$ from simulated staggered SAR range-compressed data. The black dashed line marks the useful signal level $\widehat{\sigma_2^0}_{useful}$, and the backscatter (vertical axis) is normalized such that this value is 1. The horizontal red dashed line marks the blanking threshold, which defines the $\mathcal{R}_{blank}$ interval.

While the simplest criterion for the selection of the blanking thresholds assumes equal importance on removing nadir echo and preserving useful signal, higher or lower thresholds than it indicates can be used to achieve, respectively, lower or higher nadir echo suppression. Furthermore, the simplest criterion bases itself only on the energies of the removed useful signal and nadir echoes, but there is a second mechanism by which the size of the blanking interval impacts quality of the useful signal in the final image: widening the blanking intervals causes them to overlap more along azimuth, increasing the number of consecutive samples lost in each azimuth line, which impacts the impulse response of the system in the form of elevated sidelobes. Therefore, a suggested improvement is setting an upper bound for the blanking interval size to prevent excessive degradation of the impulse response. Such a bound can be decided by considering the range separation between neighboring nadir echoes $\left|R_{nadir\ \rho,k} - R_{nadir\ \rho,k+\Delta k}\right|$, as overlapping blanking intervals occur when their width is larger than these differences. As another alternative, the staggered SAR processing proposed and analyzed in [11] could be used to avoid the elevated sidelobes.

III. Recovery of the Underlying Signal Through Interpolation of Neighboring Samples

An alternative to the thresholding-and-blanking approach is to include an additional step that exploits the azimuth oversampling of staggered SAR data to recover part of the underlying useful signal removed by the blanking of the nadir echoes. This is achieved by replacing the values of the samples corrupted by nadir echo by the best linear unbiased (BLU) estimate of their underlying useful signal based on the neighboring correlated samples in azimuth which are not (or only slightly) corrupted by nadir echo.

This additional step is called the BLU recovery. It is very similar to the BLU resampling step of the staggered SAR processing pipeline [4] but is instead executed on staggered SAR range-compressed data and interpolates into the nadir echo samples that were blanked.

Any single azimuth line of staggered SAR raw or range-compressed data can be seen as a sampling at the pulse times t_k

of a continuous-time stationary stochastic process $u(t)$ whose autocorrelation is obtained from the inverse Fourier transform of its power spectrum resulting from the azimuth antenna pattern and is negligible for any time separation greater than $\mathcal{T}$ [4]. Under these assumptions, it is possible to estimate the value of the signal $u(t)$ at any instant t through a linear combination of the neighboring correlated samples $u(t_k)\ \forall k,\ |t_k - t| < \mathcal{T}$ This process is called the BLU interpolation and consists of estimating the signal at time t through

$$\hat{u}(t) = \boldsymbol{r}^{\mathrm{T}} G^{-\mathrm{T}} \boldsymbol{u}, \tag{4}$$

where $\boldsymbol{u}$ is the vector of neighboring correlated samples, $\boldsymbol{r}$ is the vector of correlations between the neighboring samples and the estimated sample, and G is the matrix of correlations between the neighboring samples themselves [2], [4]. Furthermore, the expected estimation error is given by

$$\frac{\mathrm{E}[|\hat{u}(t) - u(t)|^2]}{\mathrm{E}[|u(t)|^2]} = 1 - \boldsymbol{r}^{\mathrm{T}} G^{-1} \boldsymbol{r}. \tag{5}$$

The BLU recovery then consists of replacing each blanked sample by an estimate of its underlying useful signal obtained by means of BLU interpolation of neighboring samples in the same azimuth line, as illustrated in Fig. 5.

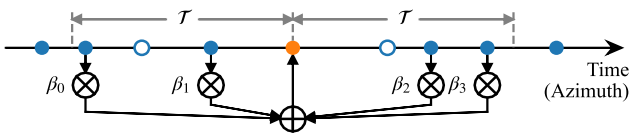

Fig. 5. Illustration of the BLU recovery of a sample (orange) through the linear combination of neighboring samples (blue) with coefficients $[\beta_0 \quad \beta_1 \quad \beta_2 \quad \beta_3] = \boldsymbol{r}^{\mathrm{T}} G^{-\mathrm{T}}$ (see (4)). Only the samples separated by less than $\mathcal{T}$ from the sample being recovered are correlated to it and used. Some samples are deliberately not used (blue, hollow), due to containing unsuitable data.

Not all neighboring samples in the same azimuth line are suitable for the being used in the BLU interpolation, though. Any neighboring sample that is itself blanked must, naturally, be ignored. Neighboring samples are also likely to still contain nadir echo, just not strong enough to warrant blanking. The BLU recovery partially copies this nadir echo over to the recovered sample, which reduces the effectiveness of the nadir echo suppression. To avoid this, a scheme equivalent to the thresholding for blanking but with a lower threshold could be used to identify these neighbors with nadir echo and have them be ignored by the BLU recovery. Also, staggered SAR raw data has gaps caused by transmit events. Range-compression around these gaps is not performed to full resolution, since only part of the echo is present. For simplicity, all these not-fully-range-compressed samples should also be ignored by any BLU recovery of neighboring samples in the same azimuth line.

Finally, since the error introduced by blanking a sample with BLU recovery is reduced according to (5), a smaller blanking threshold can be used, where samples are selected for blanking when the estimated nadir echo backscatter $\widehat{\sigma^0_\rho}_{nadir}$ is larger than the expected intensity of the error introduced, i.e., larger than $1 - \boldsymbol{r}^{\mathrm{T}} G^{-1} \boldsymbol{r}$ times the estimated underlying useful signal $\widehat{\sigma^0_\rho}_{useful}$. Note that $\boldsymbol{r}$ and G are different for each range line, as they depend on the time differences between the neighboring pulses, so different thresholds and different $\mathcal{R}_{blank}$ intervals are to be used for each range line. If the PRI sequence is periodic with period M, these values also repeat themselves every M pulses. For simplicity, one could instead compute an average threshold and use the same value for all range lines.

IV. Performance Evaluation

Let us now evaluate the performances of the proposed suppression technique with and without BLU recovery through simulations and compare them to the baseline scenario without processing for nadir echo suppression.

The simulated data have two components: the useful signal and the nadir echoes. The useful signal is simulated for a staggered SAR acquisition over a scene whose backscatter is assumed given by a TerraSAR-X image acquired near Munich. The nadir echo component for the same acquisition is simulated according to the nadir echo model presented in [9], which is also based on real TerraSAR-X data, and following the positioning dictated by the nadir echo location diagram. These components are then processed into focused images in each of the three cases: blanking with BLU recovery; blanking without BLU recovery; no processing for nadir echo suppression. The simulations were carried out with the system parameters of Tandem-L from [6], and a very long more elaborated PRI sequence (30 linear subsequences, $M = 1000$) [2], [4]. Furthermore, the strength of the nadir echoes was set such that their peak in the backscatter profile estimate described in Section II.A is 17 dB above the useful signal, a conservatively high value in comparison to the observed in two experimental TerraSAR-X acquisitions discussed in [9]. Fig. 6 shows a part of each resulting focused image containing a lake, over which the nadir echo is visible.

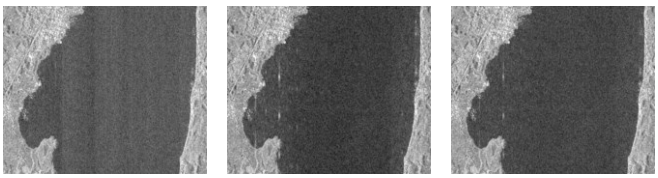

(a) (b) (c)

Fig. 6. Simulated staggered SAR focused images with nadir echo for (a) no processing for nadir echo suppression, (b) blanking nadir echoes without BLU recovery, (c) blanking nadir echoes with BLU recovery.

To compare the processing techniques, the useful signal component simulated without processing for nadir echo suppression is taken as a reference. Fig. 7 presents the error in each focused image with respect to the reference image. When no processing for nadir echo suppression is executed, this error is just the nadir echo contribution itself (cf. Fig. 7 (a)). When the processing for suppression is executed, the nadir echo component is notably reduced, but some degradation of the useful signal becomes apparent (cf. Fig. 7 (b) and (c)). Notice also that, as expected, the residual nadir echo is stronger in the case where BLU recovery is used.

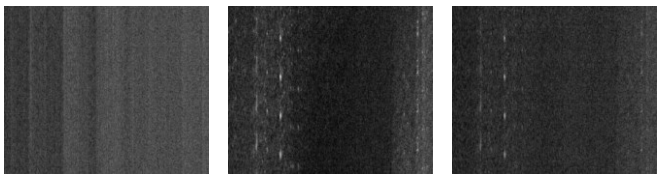

(a) (b) (c)

Fig. 7. Error with respect to the reference focused image of the simulated staggered SAR focused images with nadir echo for (a) no processing for nadir echo suppression, (b) blanking nadir echoes without BLU recovery, (c) blanking nadir echoes with BLU recovery.

The clearest manifestation of the useful signal degradation are the artifacts that appear on the lake in Fig. 6 (b) and (c) and are also clearly visible in Fig. 7 (b) and (c). They are sidelobes from strong scatterers in the city in the top left of the image that appear because of the elevation in the sidelobes of the impulse response that the processing for nadir echo suppression causes. Notice also, that, as expected, these elevated sidelobes are weaker in the case where BLU recovery is used.

Table I shows two metrics for the performance of the processing techniques: the nadir echo energy suppression and the useful signal energy suppression, which are the reduction in the energy of the nadir echo and useful signal components in the focused image caused by the processing, respectively. As expected, the case with BLU recovery presents less nadir echo suppression but also less useful signal loss.

TABLE I
PERFORMANCE METRICS FOR THE DIFFERENT NADIR ECHO SUPPRESSION APPROACHES

Method	Useful Signal Energy Suppression	Nadir Echo Energy Suppression
Just blanking	0.21 dB	3.2 dB
Blanking with BLU recovery	0.12 dB	2.0 dB

Fig. 8 presents the result of averaging along azimuth the nadir echo contribution to the image in each case. It shows that, with processing for nadir echo suppression, the nadir echo is weaker and, because the processing removes its peaks, more smoothly distributed across range.

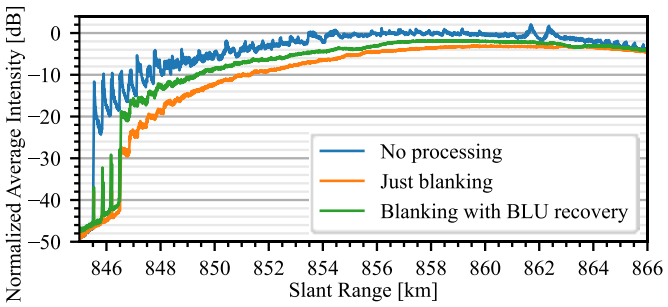

Fig. 8. Normalized intensity of nadir echo in the focused image averaged along azimuth in the case of no processing for nadir echo suppression (blue), blanking nadir echoes without BLU recovery (orange), and blanking nadir echoes with BLU recovery (green).

V. CONCLUSION

This paper uses the knowledge about the positioning and characteristics of nadir echoes in staggered SAR to propose a thresholding-and-blanking approach to nadir echo suppression. Moreover, an alternative to this method is presented where the azimuth oversampling in staggered SAR raw data is leveraged to recover part of the useful signal destroyed by the blanking, achieving less useful signal degradation at the cost of reduced nadir echo suppression. Finally, the performance of the proposed processing techniques is evaluated through simulations based on real TerraSAR-X data by comparison to the baseline case without processing for nadir echo suppression and shown to reduce the energy of the nadir echoes by 3.2 dB or 2.0 dB, depending of technique employed. Both processing techniques require no system modifications and can be readily implemented in the processing chain of planned and future SAR missions. In particular, the described processing could be implemented as an optional stage in the SAR processing chain and used to reprocess raw data in case some nadir echo is still visible and critical for some specific applications.

REFERENCES

[1] A. Moreira, P. Prats-Iraola, M. Younis, G. Krieger, I. Hajnsek, and K. P. Papathanassiou, “A Tutorial on Synthetic Aperture Radar,” *IEEE Geoscience and Remote Sensing Magazine*, vol. 1, pp. 6-43, March 2013. 10.1109/MGRS.2013.2248301.

[2] A. Moreira, G. Krieger, I. Hajnsek, K.P. Papathanassiou, M. Younis, P. Lopez-Dekker, S. Huber, M. Villano, M. Pardini, M. Eineder, F. De Zan, and A. Parizzi, “Tandem-L: A Highly Innovative Bistatic SAR Mission for Global Observation of Dynamic Processes on the Earth’s Surface,” *IEEE Geoscience and Remote Sensing Magazine*, vol. 3, no. 2, pp. 8–23, June 2015.

[3] M. Villano, G. Krieger, and A. Moreira, “Staggered SAR: High-Resolution Wide-Swath Imaging by Continuous PRI Variation,” *IEEE Transactions on Geoscience and Remote Sensing*, vol. 52, no. 7, pp. 4462–4479, July 2014.

[4] M. Villano, “Staggered Synthetic Aperture Radar,” PhD Thesis, Karlsruhe Institute of Technology, DLR-Forschungsbericht 2016-16, ISSN 1434-8454, Wessling, Germany, 2016.

[5] M. Villano, G. Krieger, M. Jäger, and A. Moreira, “Staggered SAR: Performance Analysis and Experiments with Real Data,” *IEEE Transactions on Geoscience and Remote Sensing*, vol. 55, no. 11, pp. 6617-6638, Nov. 2017.

[6] S. Huber, F. Queiroz de Almeida, M. Villano, M. Younis, G. Krieger, A. Moreira, “Tandem-L: A Technical Perspective on Future Spaceborne SAR Sensors for Earth Observation,” *IEEE Transactions on Geoscience and Remote Sensing*, vol. 56, no. 8, pp. 4792-4807, Aug. 2018.

[7] P. A. Rosen, S. Hensley, P. Agram, E. Gurrola, L. Harcke, S. Shaffer, C. Veeramachaneni, “Impact of Gaps in the NASA-ISRO SAR Mission Swath,” *Proceedings of the European Conference on Synthetic Aperture Radar (EUSAR)*, Aachen, Germany, 5-7 June 2018.

[8] M. Villano, M. Pinheiro, G. Krieger, A. Moreira, P. Rosen, S. Hensley, C. Veeramachaneni, “Gapless Imaging with the NASA-ISRO SAR (NISAR) Mission: Challenges and Opportunities of Staggered SAR,” *Proceedings of the European Conference on Synthetic Aperture Radar (EUSAR)*, Aachen, Germany, 5-7 June 2018.

[9] M. Villano and M. N. Peixoto, "Characterization of Nadir Echoes in Multiple-Elevation-Beam SAR With Constant and Variable Pulse Repetition Interval," in *IEEE Transactions on Geoscience and Remote Sensing*, doi: 10.1109/TGRS.2021.3103266.

[10] M. N. Peixoto, M. Villano and A. Moreira, "A Novel Processing Technique to Suppress Nadir Returns in Staggered Synthetic Aperture Radar," *2021 Kleinheubach Conference*, 2021, pp. 1-4, doi: 10.23919/IEEECONF54431.2021.9598397.

[11] M. Pinheiro, P. Prats-Iraola, M. Rodriguez-Cassola, M. Villano, “Analysis of low-oversampled staggered SAR data”, *IEEE Journal of Selected Topics in Applied Earth Observations and Remote Sensing*, vol. 13, 2020.